

Article

Dynamic Wind Power Plant Control for System Integration Using the Generator Response Following Concept

David Campos-Gaona *, Adam Stock, Olimpo Anaya-Lara and William Leithead

Electronic and Electrical Engineering, Wind Energy and Control Centre, University of Strathclyde, Glasgow G1 1XQ, UK; adam.stock@strath.ac.uk (A.S.); olimpo.anaya-lara@strath.ac.uk (O.A.-L.); w.leithead@strath.ac.uk (W.L.)

* Correspondence: d.campos-gaona@strath.ac.uk

Received: 31 January 2020; Accepted: 6 April 2020; Published: 8 April 2020



Abstract: In this paper, a novel concept to integrate High Voltage Direct Current (HVDC)-connected offshore wind power plants with the onshore grid is presented. The concept makes use of a holistic wind farm controller along with a fully instrumented conventional synchronous generator at the point of common coupling. In our approach, the wind farm is able to replicate the natural response of the generator to a system, even enabling the wind farm to reproduce, in a scaled up manner, a range of ancillary services without having to rely on indirect frequency measurements which are prone to noise and delays. Simulation results are presented to validate the proposed solution.

Keywords: wind farm control; synthetic inertia; ancillary services; grid integration; wind energy; HVDC transmission; offshore wind

1. Introduction

Wind power penetration in modern power systems brings new challenges regarding the controllability and behaviour of wind power plants. Nowadays, it is not satisfactory for wind power plants to focus solely on power production. Instead, it is expected that large offshore and onshore wind farms instead become a “virtual generation plant” that behaves in a similar way to conventional synchronous generators. As such, the power output of wind farms is no longer expected to be driven only by the incoming wind speed—rather, the power should be adjusted as required by the Transmission System Operators (TSOs). To do this, new wind farm controllers are required to provide not only the maximum possible wind power output, but also to provide ancillary services to the grid, such as curtailment, frequency support and voltage regulation.

Although very few details are publicly available regarding their design and performance, modern wind farms are fitted with state-of-the-art supervisory controllers that provide a variety of functions, enabling the control of effective active and reactive power and implementation of all functionalities required by grid codes at the Point of Connection (PoC). The current state of the art for Wind Power Plant Control (WPPC) is to let turbines operate normally at their individual optimal settings and to distribute proportionally to their downregulation set-points. Other control functionalities include power curtailment, balance control, power rate limits (increase only) and delta control [1]. The focus of recent WPPC research is provided in [2]. It has mainly been focused on maximising power production, steady state load mitigation and optimised downregulation, using both centralised and distributed approaches; however, the contribution to grid operation has been almost totally overlooked. Regarding the provision of Ancillary Services (AS), significant research has been conducted dealing with frequency support [3], including the impact of turbine frequency support on the loads using a full-scale demonstration setup.

In this research, a holistic and hierarchical control approach, built upon the Power Adjusting Control (PAC) concept [4–7], is used. This control approach allows a wind power plant to provide a full range of ancillary services, including inertial response at the wind farm level, rather than at the single turbine level. Figure 1 shows the PAC concept applied to a wind turbine where an augmentation is added to the full envelope controller of the wind turbine to regulate its power output. At the wind farm level, the power output of each turbine is regulated by a wind farm controller to provide an aggregated response (the PAC controller is analyzed in detail in Section 2).

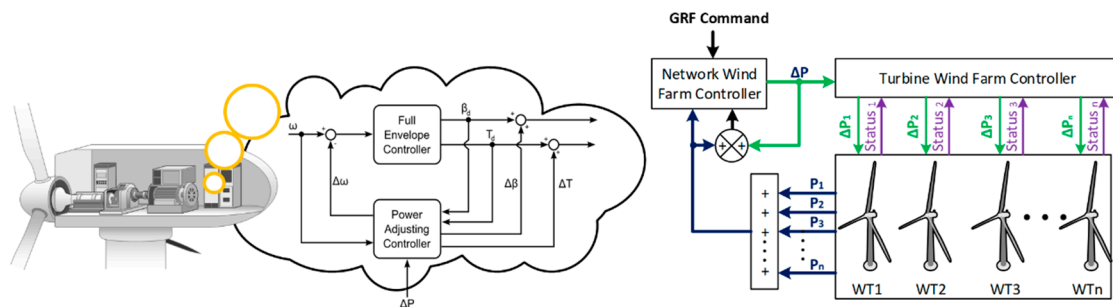


Figure 1. The power adjusting control concept at turbine and wind farm level.

However, key issues with respect to the provision of ancillary services, namely the power system event detection and coordination with the offshore and onshore substations, require accurate and fast information of the behaviour of the AC frequency of the grid. As an alternative to direct grid frequency measurements used currently in the power industry, which is prone to high noise, a lack of accuracy and delay [8–10], this research uses a fully instrumented small/medium synchronous generator at the wind power plant point of connection. Additionally, by slaving the wind farm (or more accurately the wind farm controller) to the generator, the wind farm also provides ancillary services that are similar to the generator, but greatly scaled up. This methodology is referred in this research as the Generator Response Following (GRF) concept. A schematic diagram of the GRF concept is presented in Figure 2. The GRF controller uses feedforward systems to provide an immediate dynamic response from an High Voltage Direct Current (HVDC)-connected wind farm when communication delays prevent an immediate response from a distant offshore wind farm.

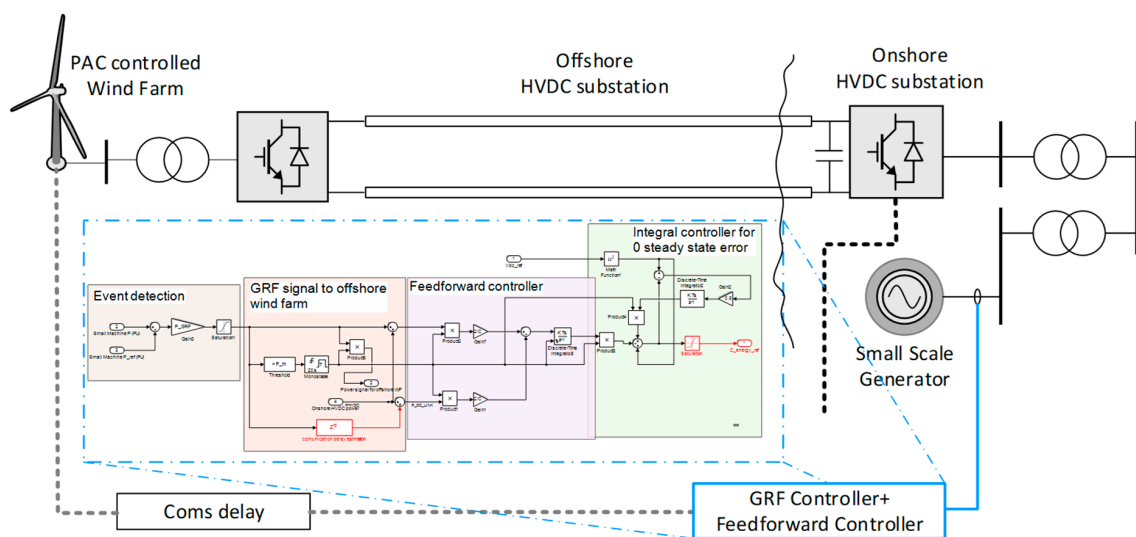


Figure 2. The Generator Response Following concept in a HVDC connected offshore wind farm.

The simulation results of using PAC controllers along with the GRF concept demonstrate the feasibility of the system for different dynamic conditions. These results are analyzed and discussed in detail in this work.

The structure of this paper is as follows: Section 2 explains the theory behind the PAC controller. Section 3 describes the Generator Response Following concept. Section 4 presents the design methodology of controllers for HVDC systems in order to apply the GRF concept to provide immediate response during frequency events in the power grid. Section 5 presents the simulation results of the GRF concept connected to a multi-machine system and analyses the performance of the GRF for different governor settings for the small-scale generator. Finally, Section 6 presents the conclusion of this work.

2. The PAC Controller

In order to provide wind farm control, wind turbines need to be able to alter their operation away from their usual strategy. In order to alter their operation, some form of control beyond typical rotational speed constrained max power coefficient tracking is required. Not all wind turbines have this capability and those that do are typically controlled by Original Equipment Manufacturer (OEM)-designed controllers that are not readily available to the academic community. The PAC was therefore designed to meet the following criteria:

1. The PAC should be applicable to all variable speed pitch regulated wind turbines without requiring alteration to the wind turbine's full envelope controller;
2. No knowledge should be required of the wind turbine's full envelope controller (as this is rarely available);
3. No matter how defined, the PAC must allow the operator to vary the power output of the wind turbine by an increment ΔP ;
4. The wind turbine's power output should be able to be altered quickly and accurately by the PAC;
5. If there are any different modes of operation, then the PAC must switch between these smoothly;
6. The performance of the full envelope controller must not be compromised through the addition of the PAC, including taking into account any gain scheduling.

Full details of the design of the PAC can be found in [6,11]. In this section, a brief explanation of how the PAC operates and how it meets the requirements outlined above will be provided.

A diagram of the PAC is provided in Figure 3. A simplified overview of the process used by the PAC to increment the power by ΔP , which is useful for explaining the process, is presented in Figure 4.

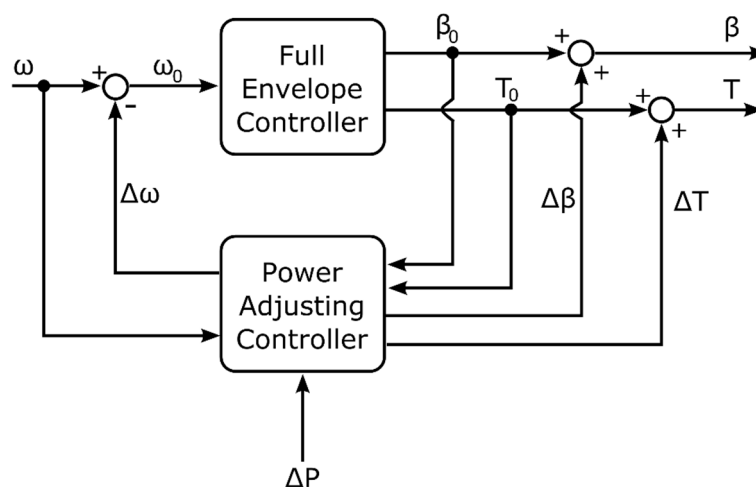


Figure 3. Power Adjusting Control (PAC) schematic diagram.

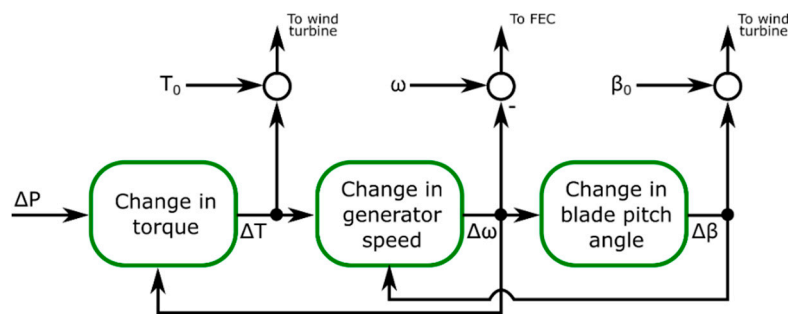


Figure 4. Simplified PAC process.

Note that throughout this section similar subscripts will be used, whereby Δx indicates an increment from the PAC in signal x , x_0 indicates the value of signal x either produced by or received by the full envelope controller, and x with no subscript indicates the sum of Δx and x_0 .

The PAC changes the power output of a wind turbine through an increment to the torque ΔT that is added to the torque demand of the full envelope controller, T_0 , to give the total torque demanded from the generator T . The change in torque compared to that if the PAC had not been used induces a change in the generator speed. Using a simple first order approximation of the wind turbine dynamics, an estimate of the change in generator speed caused by the PAC's operation, $\Delta\omega$, is calculated. The change in generator speed is subtracted from the measured generator speed, ω , with the result ω_0 becoming the new input to the full envelope controller. Without any further control action, whilst the change in power may be correct, the wind turbine's generator speed would continue to change—an undesirable result. Hence, an increment $\Delta\beta$ is added to the pitch demand from the full envelope controller, β_0 , that changes the aerodynamic torque of the turbine rotor. By using an appropriately gain scheduled Proportional Integral (PI) controller with anti-wind up limits, the change in pitch angle minimizes the change in generator speed. Note that the torque action is fast, allowing fast alteration of the power, whilst the time constant of the wind turbine dynamics from generator torque to generator speed are slow, and so only a slow change to the pitch angle is required to ameliorate the changes in generator speed.

Whilst the change in torque is dependent upon the change in generator speed and the change in generator speed is dependent upon the change in pitch angle, it is important to note that any feedback around the full envelope controller is very weak—the PAC is almost exclusively feedforward. The feedforward property of the PAC means that the feedforward gain of the Full Envelope Controller is unaffected by the presence and operation of the PAC.

2.1. Provision of Positive and Negative Increments in Power

The PAC can be used to provide either a positive or a negative change in power. If the change in power is negative, then an equilibrium operating point (which is a point whereby the turbine rotor torque and the required generator torque can be matched for a given wind speed) will be available and, as such, the change in power can be held indefinitely. For an increase in power, there may or may not be an equilibrium operating point for the given wind speed. In cases where the turbine is operating above the rated wind speed (typically above around 12 m/s), the full envelope controller utilizes the pitch actuators of the blades to decrease the aerodynamic torque of the rotor in order to maintain a suitable generator and rotor speed. In the case of the above rated wind speed operation, it is possible to reduce the pitch angle to increase the rotor torque and hence provide an increase in power for a prolonged period. The limitations on how long the increase in power can be maintained therefore become those of mechanical loads on the turbine structures and drivetrain (both fatigue and extreme loads should be considered) and of the thermal loads on the electrical components.

In below rated wind speed operation, a wind turbine is typically operated at its maximum power coefficient, so there is not a suitable equilibrium operating point that can be achieved through pitching

the turbine blades. With a positive increment in power, the rotor is therefore slowed as kinetic energy is converted from the rotor momentum into electrical energy. The duration for which an increase in power can be maintained therefore becomes a function of the magnitude of the desired increase in power, the inertia of the wind turbine rotor and drivetrain, and the operating strategy (including the proximity to the aerodynamic stall region). For example, for a 5MW wind turbine, the duration for which such increases could be maintained was found to typically be around 10 to 15s for wind speeds above 8 m/s. [4,6]. The amount of time that power can likely be increased for increases with turbine size. Work by Jamieson [12] on the scaling of wind turbines can be used to give estimates for the increase in energy stored in the blades. Jamieson gives a power law exponent for a mass of 2.29 and for a tip speed of 0.28. These combine to give a power law exponent for inertia of 4.58 and hence a power law exponent for energy stored in the blades of 3.14, slightly higher than cubic. Of course, the operating strategy and the aerodynamics of the particular blades used also factor into the duration that power can be increased for and so it is difficult to exactly quantify the increase in time with increase in turbine size.

2.2. Meeting of Design Criteria

With reference to the design criteria listed previously, the PAC clearly meets the requirements as detailed below:

1. The PAC requires just pitch and torque actuation and so any variable speed pitch regulated machine is suitable, i.e., it is generic and not turbine specific;
2. The design of the PAC explicitly does not interfere with or require knowledge about the operation of the Full Envelope Controller;
3. The PAC will provide any value for the change in power, i.e., it is entirely flexible and not designed with just a single task in mind;
4. By implementing the increment in power directly through the torque actuation, the PAC is able to respond quickly, limited only by the generator (typically < 0.01 second time step);
5. The PAC operates in the same manner across the operating envelope and so there are no switching point;
6. Any feedback around the full envelope controller is very weak (the PAC is effectively a feedforward controller) and so the feedforward gain of the full envelope controller is unaffected by the presence of the PAC.

2.3. Supervisory Control

It is clearly important that the PAC does not allow the wind turbine to operate outside of a safe operating envelope. A safe operating envelope could be defined in many different ways; however, a typical envelope would be that constrained by a minimum rotational speed, a maximum rotational speed, a set minimum torque as a function of rotational speed and a set maximum torque as a function of rotational speed. The PAC is also required to be able to “recover” the operating point back to normal operation (i.e., operation without the PAC). Details of how such limits are achieved can be found in [6]. For the purposes of the work presented here, it can simply be stated that the PAC will not permit operation outside of a safe operating envelope and will recover operation back to normal operation if a limit is encroached upon.

3. The GRF Concept

In the event of power system frequency excursions, synchronous plants naturally provide inertia and other frequency support services through governor action. In order to do this, they rely on direct measurements of the power system frequency by analogue (Watt flyballs) or electronic means. Although these frequency measurements are prone to errors and delays, the large time constants (i.e., seconds) of the closed loop controller of the governor makes it possible to realize proper control.

Additionally, during frequency excursions, the initial power output of the generators is not dictated by the governors, but instead by the kinetic energy dynamics of the generator, meaning that no accurate frequency measurements are needed here either. However, if the power dynamics of a power plant are not dictated by the natural behaviour of rotating elements, but instead are commanded by a control law (such as in the case of a PAC-controlled wind farm), then the delays and inaccuracies in frequency measurement would make it impossible to command the wind farm power output to accurately emulate the behaviour of a synchronous generator during frequency excursions. Depending of the size of the wind farm, these inaccuracies and delays are a potential source of instability in the power network.

Contrary to direct frequency measurements, this paper proposes an innovative method where a fully instrumented small/medium synchronous generator is installed at the point-of-connection (PoC) of the wind farm with the rest of the power grid, as shown in Figure 5.

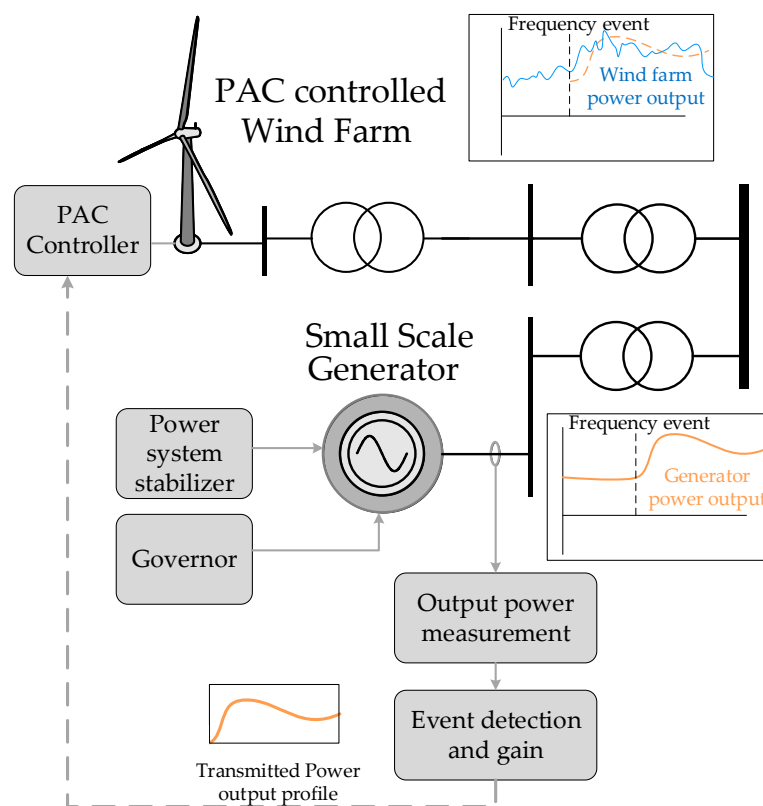


Figure 5. Generator Response Following (GRF) concept schematic.

The small synchronous generator will be able to provide all ancillary services (assuming it has a Power System Stabilizer (PSS) and Automatic Voltage Regulator (AVR), inertia, governor droop control, reactive power, reserve, and curtailment functionality). By slaving the power output controller of the wind farm to the power output of the generator, the wind farm will emulate the synchronous generator behaviour and provide similar Ancillary Services (AS) at far greater accuracy than by using frequency measurements. Additionally, this master–slave controller will ensure that the power demand to the wind farm controller is set as required to deliver similar ancillary services as the small/medium scale generator and will also determine the degree to which the wind farm can mimic the small/medium generator behaviour.

4. VSC-HVDC Connected Wind Farm System Using the GRF Concept

Figure 6 shows a schematic of the system under study, whereby a large offshore wind farm is connected to the power grid through a Voltage-Source Converter (VSC)-HVDC. The GRF concept is

used to detect a system frequency event and coordinate the action of a PAC-controlled offshore wind farm. The GRF controller uses feedforward systems to provide an immediate dynamic response from a VSC-HVDC-connected wind farm when communication delays prevent an immediate response from a distant offshore wind farm.

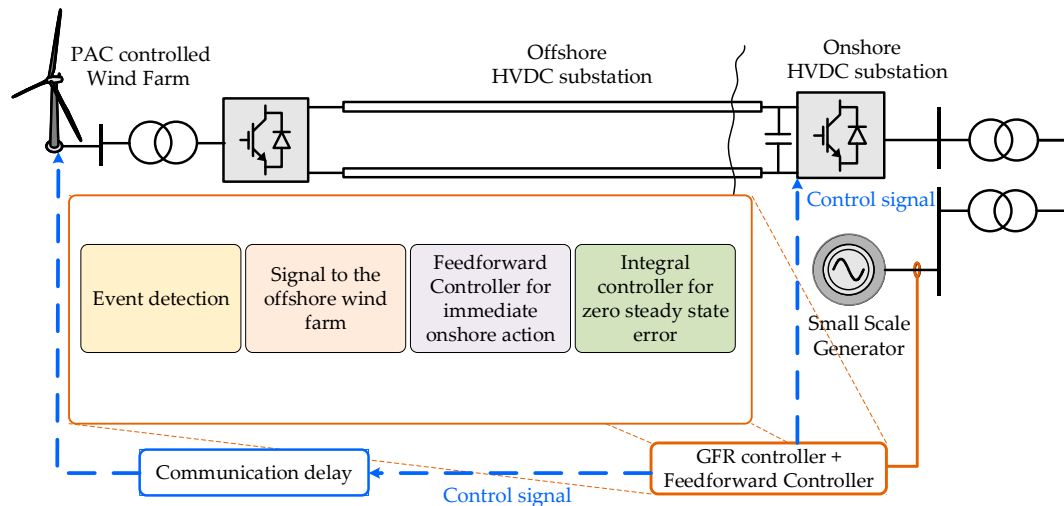


Figure 6. The Generator Response Following concept in a VSC-HVDC connected offshore wind farm.

4.1. Use of 2DF IMC for Improved Disturbance Rejection in the HVDC DC Voltage Controller

The use of feedforward controllers to provide an immediate response in cases of frequency excursions requires the use of energy stored in the DC capacitors of the HVDC link. To do so in a fast and accurate manner, an additional control loop has to be added to the DC voltage controller. This additional control loop commands the DC voltage to follow a specific “shape” which is then translated in a release of stored energy from the HVDC capacitors. This energy follows the natural power output of a synchronous generator during a frequency excursion for a period of hundreds of milliseconds until the delayed action of the offshore wind farm takes place. Nevertheless, having precise control of the DC voltage during this event is not a trivial task because of the poor disturbance rejection characteristics of the DC of the HVDC system plant (i.e., a plant with a pole in the origin [13]). This is because the delayed action of the offshore wind farm is reflected as a sudden disturbance in the control loop regulating the DC voltage, which, if not dealt with properly, affects the capability of the onshore HVDC station to mimic the response of the small/medium-size generator. To deal with this problem, the robust control technique of the two degrees of freedom internal model control is used.

The internal model control (IMC) technique uses the “internal model” philosophy that states that a control action over a plant can be achieved only if the control system includes, either implicitly or explicitly, some representation of the process to be controlled [14–16]. Figure 7 shows the structure of the IMC.

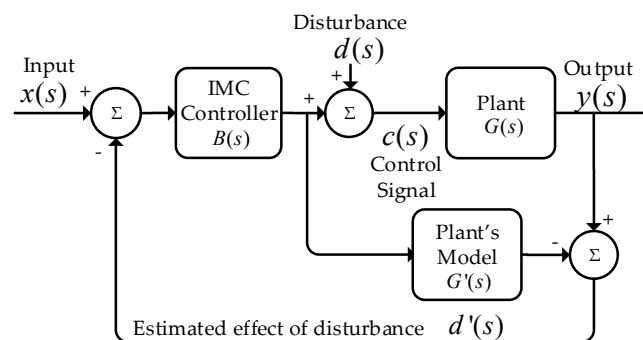


Figure 7. Internal model control (IMC) controller [14–16].

As seen in the model of the plant to be controlled $G'(s)$ is to be an exact representation of the plant itself $G(s)$ and considering that no disturbance is present, then the estimated effect of disturbance $d'(s)$, resulting from the difference between the plant output and the plant model output, becomes zero and the close loop system becomes equal to the open loop system. On this condition, an IMC controller of the type $B(s) = G'^{-1}(s)$ implies a perfect theoretical control then. However, such ideal control cannot be implemented for two main reasons:

1. The requirement for pure differentiators, (in the case that the model of the plant is proper, which is true for any physical process);
2. Infinitely large excursions of the manipulative variable for infinitely small high frequency disturbances (which cannot be implemented realistically in any digital or analog controller).

For realizable control, the IMC structure introduces a low pass filter $L(s)$ in cascade to the IMC controller. The filter is designed to add poles to $G(s)$ in order to make the controller transfer function proper. The filter $L(s)$ is usually of the type

$$L(s) = \left(\frac{\alpha}{s + \alpha} \right)^n \quad (1)$$

where the order of the filter n is chosen accordingly to the order of $G(s)$, and α is regarded as the closed loop bandwidth of the filter, for a first order filter.

The IMC controller has the advantage of having its controller parameters related in a unique manner to the model parameters, with the variable α being the only user-selected variable.

4.2. The Need of an Additional Degree of Freedom for Poorly Damped Processes

When there is a reference change in a closed loop control system, the mathematical damping of the controller combines with the physical damping of the process; this combination smooths out the process's response to a set-point change. However, if an unexpected load affects the process, a set point tracking controller will tend to overreact and cause the process output to oscillate unnecessarily. This is because a set point tracking controller does not play a significant role in determining how the process reacts to a disturbance; as such, the load disturbance rejection of the closed loop system, even with the use of a fast IMC or PID controller, is still determined by the natural disturbance rejection capabilities of the process (see Figure 8).

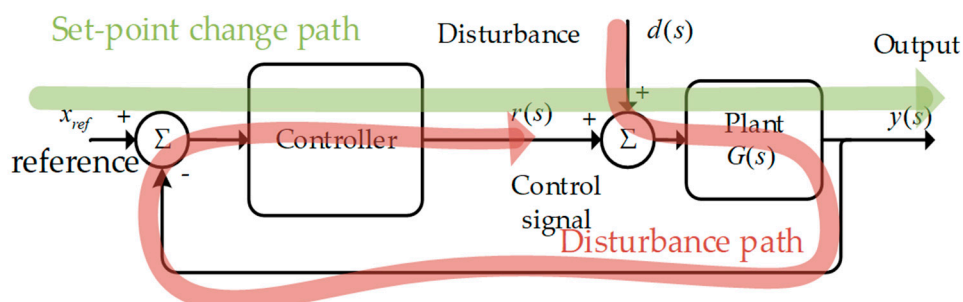


Figure 8. Set-point and disturbance paths in a closed loop controller.

The performance of the IMC controller can be provided with extra robustness by adding an inner feedback loop to the plant, which provides an additional degree of control freedom to speed up the load disturbance rejection. This additional control loop is used to speed up the natural response of the plant by moving the pole of the plant away from the origin on the negative side of the real axis. The configuration of the additional control loop is shown in Figure 9.

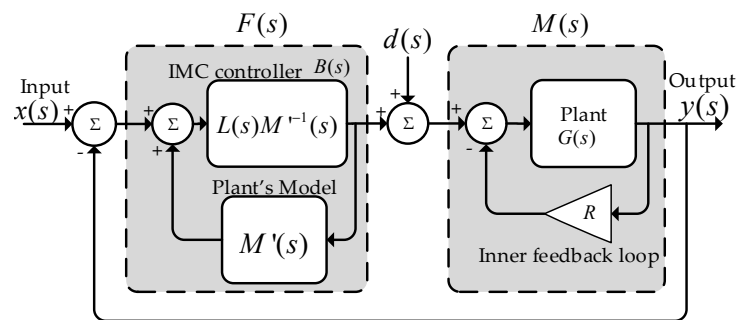


Figure 9. The two degrees of freedom IMC configured as a PI controller.

By adding a second degree of control freedom, the transfer function of the improved plant $M_{dc}(s)$ becomes

$$M(s) = \frac{G(s)}{1 + G(s)R} = \frac{1}{G^{-1}(s) + R} \quad (2)$$

where $M(s)$ is the new transfer function of the plant augmented with an inner feedback loop gain R .

This IMC with an extra degree of control freedom is especially useful for the poorly damped systems of the inverter, such as the DC circuit of the HVDC system.

The processes to be controlled using the two degrees of freedom IMC controller are the dq currents and the DC voltage. The transfer functions of these processes are given by a first order transfer function, implying a first-degree filter for their respective IMC controller. Under this consideration, the transfer function of the IMC controller $F(s)$ (considering that $M'(s)$ is the model of $M(s)$) is shown in Equation (3)

$$F(s) = \frac{B(s)}{1 - B(s)M'(s)} = \frac{L(s)M'^{-1}(s)}{1 - L(s)M'^{-1}(s)M'(s)} = \frac{\alpha}{s}M'^{-1}(s) \quad (3)$$

The additional degree of freedom is chosen, in each controller case, to make the process dynamics as fast as the controller dynamics. This allows the load disturbance rejection to be as fast as the controllers' closed loop dynamics. To achieve this, the pole R is set in the inner feedback loop to match the pole of the IMC controller in the transfer function from the disturbance $d(s)$ to the output signal of the plant $y(s)$, which is:

$$\frac{y(s)}{d(s)} = \frac{M(s)}{1 + F(s)M(s)} = \frac{M(s)}{1 + (\alpha/s)M'^{-1}(s)M(s)} = \left(\frac{s}{s + \alpha}\right) \frac{1}{G^{-1}(s) + R} \quad (4)$$

If R is chosen appropriately, Equation (4) can be reduced to

$$\frac{y(s)}{d(s)} = \left[\left(\frac{s}{s + \alpha}\right) \frac{K}{s + \alpha} \right] = K \left[\frac{s}{(s + \alpha)^2} \right] \quad (5)$$

where K is a constant.

As can be seen in Equation (5), the load disturbance $d(s)$ is damped with the same time constant as the closed loop control.

The IMC controller closed loop bandwidth α is chosen accordingly such as the rise time t_r needed for the output signal $y(s)$, which, for a first order system, is given by following the formula that defines the relationship between bandwidth and rise time [16], this is:

$$\alpha_p \approx \frac{0.35}{t_{r_p}} \text{ (Hz)} \text{ or } \alpha_p \approx \frac{2.2}{t_{r_p}} \text{ (rad)} \quad (6)$$

4.3. The Two Degrees of Freedom IMC Controller Applied to DC Voltage Control in an HVDC System

The DC plant equation of the HVDC system is defined as:

$$C \frac{dv_{dc}}{dt} = i_{dc_wf} + i_{dc} \quad (7)$$

where i_{dc_wf} is the DC current provided by the offshore HVDC converter to the DC circuit, i_{dc} is the DC current absorbed by the onshore HVDC and C is the capacitance of the DC circuit. The average value of i_{dc} can be represented in terms of the AC currents and modulator signals. In the dq reference frame, this is:

$$i_{dc} = \frac{3}{4} (m_{d_inv} i_d + m_{q_inv} i_q) \quad (8)$$

where m_{d_inv} and m_{q_inv} are the d and q components of the inverter modulator signal, i_d and i_q are the d and q components of the AC current circulating between the onshore HVDC station and the onshore AC grid. The equation of the ac circuit of the onshore HVDC, in terms of modulator signals, is thus given by [13]:

$$\left. \begin{aligned} \frac{v_{dc}}{2} m_d = v_{d_inv} &= r i_d + L \frac{di_d}{dt} - L \omega i_q - v_d \\ \frac{v_{dc}}{2} m_q = v_{q_inv} &= r i_q + L \frac{di_q}{dt} + L \omega i_d - v_q \end{aligned} \right\} \quad (9)$$

where r and L are, respectively, the equivalent resistance and inductance between the onshore HVDC station and the onshore grid, v_{d_inv} and v_{q_inv} are the dq components of the average voltages generated by the onshore HVDC station, v_d and v_q are the dq components of the onshore grid AC voltage. Substituting Equations (8) and (9) in Equation (7) and assuming the grid voltage is aligned to v_d (i.e., $v_q = 0$), the following expressions for i_{dc} and the onshore HVDC DC power P_{dc} are obtained:

$$i_{dc} = \frac{3R}{2v_{dc}} (i_d^2 + i_q^2) + \frac{3L}{2v_{dc}} \left(i_d \frac{di_d}{dt} + i_q \frac{di_q}{dt} \right) - \frac{3}{2v_{dc}} (v_d i_d) \quad (10)$$

$$i_{dc} v_{dc} = P_{dc} = \frac{3R}{2} (i_d^2 + i_q^2) + \frac{3L}{4} \frac{d}{dt} (i_d^2 + i_q^2) - \frac{3}{2} (v_d i_d) \quad (11)$$

Equation (11) shows that the DC side power of the onshore HVDC is composed of the sum of the resistive losses in the ac side ($3(i_d^2 + i_q^2)R/2$), plus the inductor energy of the onshore HVDC ($\frac{3L}{4} \frac{d}{dt} (i_d^2 + i_q^2)$), plus the AC active power ($\frac{3}{2} (v_d i_d)$).

Neglecting the resistive losses and the stored energy in the inductor, it is found that the equation describing the dynamics of the DC voltage can be simplified as:

$$\begin{aligned} C v_{dc} \frac{dv_{dc}}{dt} &= v_{dc} (i_{dc_wf} + i_{dc}) \rightarrow \\ C v_{dc} \frac{dv_{dc}}{dt} &= P_{wf} + P_{dc} \rightarrow \\ \frac{C}{2} \frac{dv_{dc}^2}{dt} &= P_{wf} + \left(-\frac{3}{2} (v_d i_d) \right) \end{aligned} \quad (12)$$

Equation (12) is non-linear; however, the output variable of the DC plant is selected to be the square of the capacitor voltage (i.e., a representation of the energy of the capacitor). Thus, selecting the square of the capacitor voltage to be $w = v_{dc}^2$ and considering the power coming from the offshore wind farm, P_{wf} , an external disturbance (and therefore not taken into account during the calculation of the DC voltage controller), then the transfer function of the DC-plant can be presented as:

$$-\frac{w(s)}{i_d(s)} = -G_w(s) = -\frac{3v_d}{Cs} \quad (13)$$

As seen in Equation (13), $-G_{dc}(s)$ has a pole at the origin, which makes it susceptible to external disturbances.

Following the procedure for designing a two degrees of freedom IMC controller, an inner feedback loop of gain R_w is added to the DC plant to add active damping to G_w (i.e., a second degree of freedom, as shown in Equation (2)). This is:

$$-M_w(s) = -\frac{G_w(s)}{1 + G_w(s)R_w} = -\frac{3v_d}{Cs + 3v_dR_w} \tag{14}$$

The inner feedback loop is implemented to the DC plant by means of making the input signal to the DC plant equal to

$$i_d(s) = i_d'(s) - w(s)R_w \tag{15}$$

where $i_d'(s)$ is the output of the IMC current controller $F_w(s)$, which, using Equation (3), becomes

$$F_w(s) = \frac{\alpha_w}{s} (-)M_w^{-1}(s) = \frac{\alpha_w}{s} \left(-\frac{3v_d}{Cs + 3v_dR_w} \right)^{-1} = -\left(\frac{\alpha_w C}{3v_d} + \frac{\alpha_w R_w}{s} \right) \tag{16}$$

where α_w is the bandwidth of the closed loop system of the $v_{dc}^2 = w$ control system.

From Equation (16) the controller constants can be calculated as:

$$\begin{aligned} Kp_w &= \frac{\alpha_w C}{3v_d} \\ Ki_w &= \alpha_w R_w \end{aligned} \tag{17}$$

Now R_w can be selected to match the pole of $M_w(s)$ with the pole of $F_w(s)$ on the transfer function from the disturbance $d_w(s)$ (in this case P_{wf}) to the output of the plant $w(s)$. The process to do this is presented in Equation (4). Thus, selecting R_{dc} to have the value of

$$R_{dc} = \frac{1}{3} \frac{\alpha_{dc} C}{v_d} \tag{18}$$

it can be shown that the relationship $v_{dc}^2(s)/P_{wf}$ becomes

$$\left(\frac{v_{dc}^2(s)}{P_{wf}} \right) = \left(\frac{2s}{(Cs + 3v_d G_{dc})(s + \alpha_{dc})} \right) = \left(\frac{2s}{C(s + \alpha_{dc})^2} \right) \tag{19}$$

As seen in Equation (19), a power step of magnitude $|P_{wf}|$ is rejected by the DC plant with the same time constant as the closed loop controller, which, in turn, depends on α_w . Figure 10 shows the DC voltage control loop.

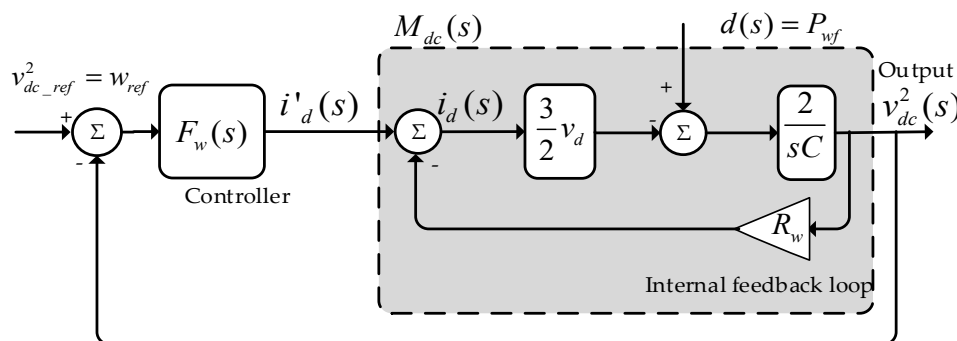


Figure 10. DC voltage control loop.

4.4. The Feedforward Controller for the GRF Concept

The feedforward controller is composed of several stages to implement the GRF concept in the offshore wind farm. These stages are described in this section.

4.4.1. Event Detection

This stage compares the power output of the small/medium scale generator against its power output set point. Whenever the output power of the generator is higher than its set point this could be an indication that a frequency event has happened. However, in order to differentiate between a steady-state governor action and a frequency excursion, a threshold to activate the GRF signal is incorporated in the detection mechanism. This threshold is user selectable and should be defined based on the droop constants of the small/medium scale generator. A small droop constant makes the generator governor more sensitive to steady state frequency variations. A large droop constant makes the governor less sensitive to frequency variations, which in turn implies less steady-state deviation from its power set point.

4.4.2. The GRF Signal to Offshore Wind Farm Stage

After a positive detection of a frequency excursion, the signal to the offshore wind farm to produce extra power (following the behaviour of the small/medium scale generator) is sent to the master PAC controller of the offshore wind generators. The duration of the GRF signal (i.e., the time over which the offshore wind farm power output should follow the behaviour of the small/medium scale generator) is a user-configurable variable. This duration is selected based on the reasonable synthetic power output capabilities of the offshore wind farm.

4.4.3. The Feedforward Controller

The feedforward controller discharges the DC voltage of the HVDC link capacitors to provide an immediate synthetic inertia response following the “shape” of the power output of the small/medium size generator. The feedforward controller modifies the set point of the controller that controls the energy in the DC capacitors (i.e., the voltage controller) in order to reproduce the requested power output of the GRF signal. The feedforward controller relies on the robust two degrees of freedom IMC controllers deployed in the HVDC DC system to faithfully represent the power dynamics needed. As explained previously, the DC voltage controller of the HVDC system has increased load disturbance rejection capabilities thanks to the use of the 2DF-IMC controllers. The feedforward controller also considers the delayed energy provision from the wind farm in order to reduce the effects of such energy on the instantaneous value of the DC voltage. Since any error between the DC voltage reference and the real DC signal implies an inaccurate representation of the instantaneous synthetic inertia provision from the HVDC, the 2DF-IMC structure plays a key role in accurately controlling the DC voltage in the presence of sudden input disturbances.

4.4.4. Integral Controller for Zero Steady State Error

The integral controller objective is to bring the DC voltage back to its set point level after the GRF action. The speed of response of this controller is much slower than the feedforward controller. As such, the feedforward controller can take priority during frequency excursions without being affected by the dynamics of the integral controller. After the GRF action is complete, the integral controller restores the DC voltage to the nominal value. Additionally, this section of the controller contains a saturation element to limit the energy extraction from the DC capacitor.

The different stages of the feedforward controller deployed in Simulink are shown in Figure 11.

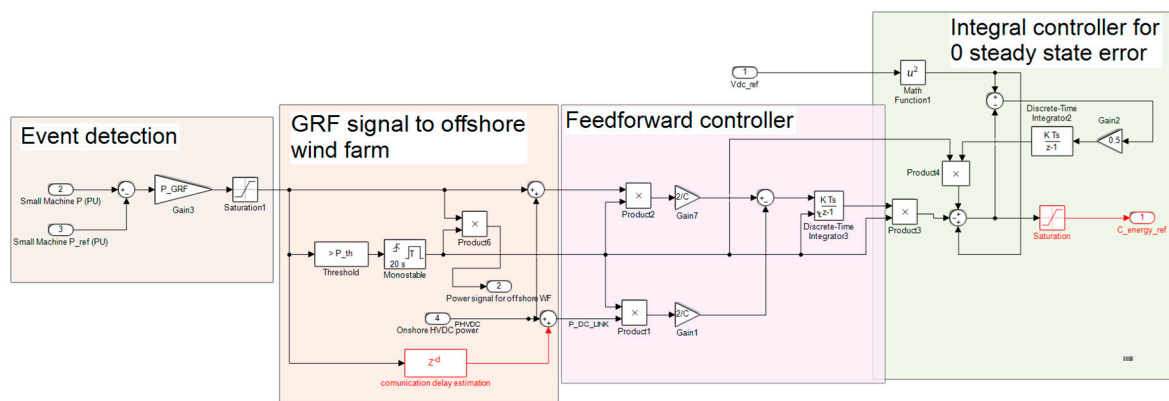


Figure 11. The GRF feedforward controller.

4.5. Simulink Test Multi-Machine System Model for Frequency Excursions

A complex multi-machine system consisting of four generators, governors, transformers, transmission lines and VSC-HVDC converters is developed to create a network for testing the Generator Response Following concept. The multi machine model consists of three high power generators and one medium-sized generator. The power output of the medium-sized generator is used to command a PAC emulator at the offshore wind farm for synthetic inertia using the Generator Response Following concept. The PAC-based wind farm emulator is connected to a VSC-HVDC transmission system controlled by two degrees of freedom internal model controllers. The wind farm is composed of an aggregated model of a type 4 Permanent Magnet Synchronous Generator (PMSG) wind turbine. Figure 12 shows a picture of the developed Simulink model.

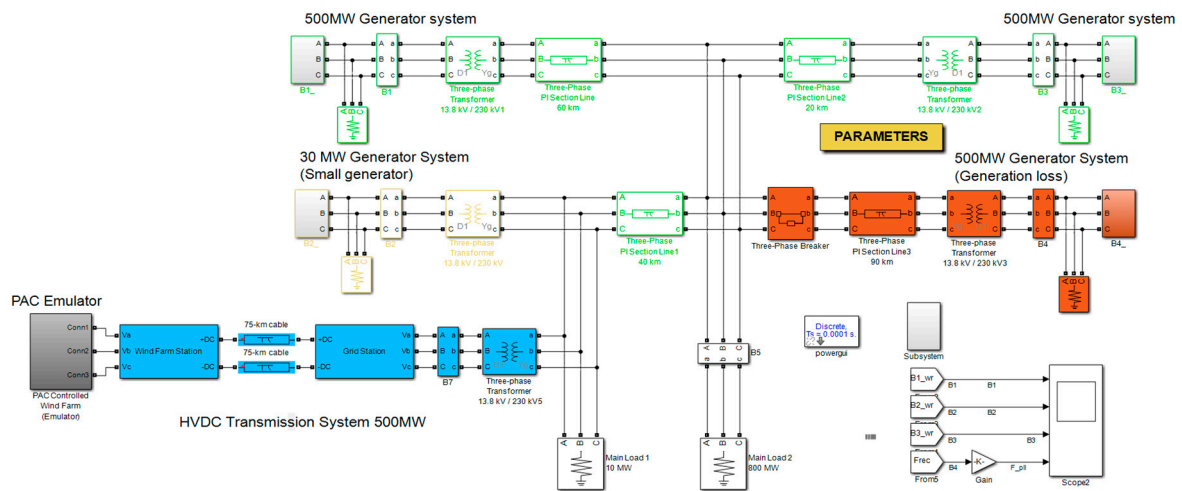


Figure 12. Multi-machine model for Generator Response Following concept testing.

The multi machine AC grid runs from an initial state condition where all the machines are in a steady state, providing a significant fraction of its power to the grid loads. The initial condition for the multi-machine system was obtained by running a power flow analysis. During the power flow analysis, the HVDC system was substituted with a generic 500MW machine to obtain its steady state power injection. Once the steady state conditions were obtained, these were embedded within the B2B system, resulting in a full steady state operative condition for the simulated grid. The excitation of each machine system was calculated to provide 1 PU of AC voltage at the terminal of the generator.

5. Evaluation of the Generator Response Following Concept

5.1. Evaluation of the Generator Response Following Concept Assuming Constant Wind Speed and No Communication Delay

Figure 13 shows the performance of the multi-machine test model when a sudden loss of a generator at $t = 10$ s affects the frequency of the system.

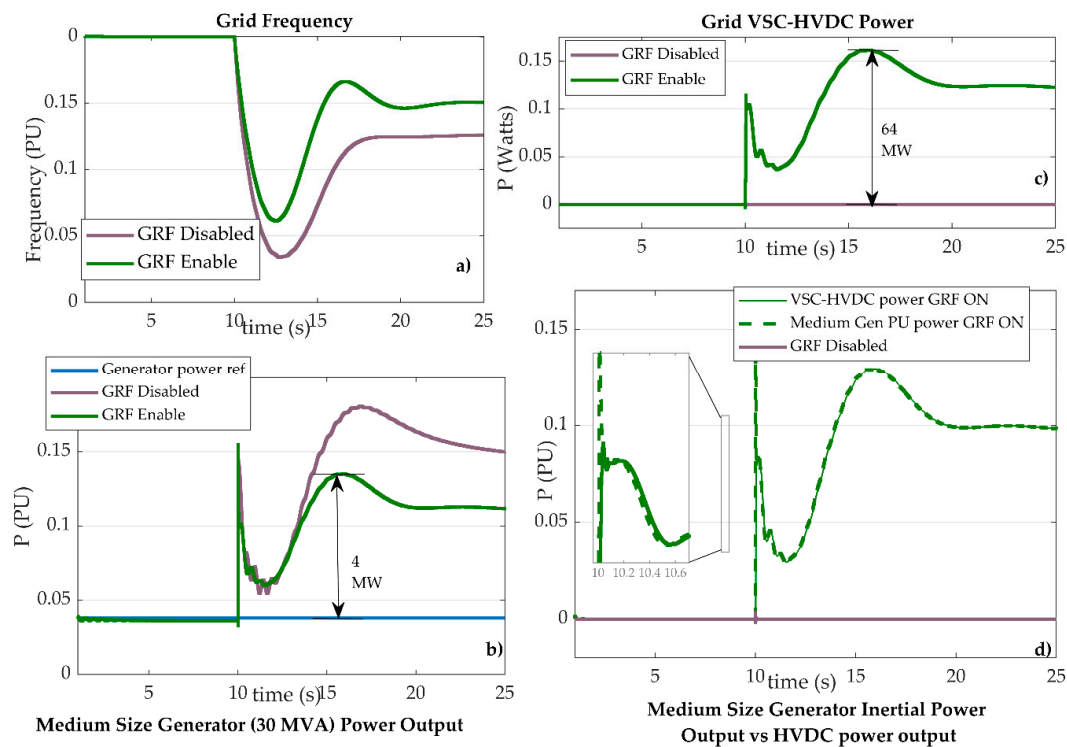


Figure 13. Behaviour of the multi-machine model for Generator Response Following concept control, assuming no communication delay.

Figure 13 includes the behavior of the test model when Generator Response Following (GRF) is disabled (purple plots) and when GRF is enabled (green plots). As seen in Figure 13a, the frequency rate of change and the drop in the system frequency is reduced when GRF is enabled. Figure 13b shows the power output of the medium size generator during the frequency excursion. As seen in Figure 13b, the natural inertia response of the small machine generates a peak of extra power above the power reference of the machine (blue line). When GRF is enabled, the magnitude and shape of extra power generated by the small generator is magnified 16 times by the VSC-HVDC station, as seen in Figure 13c. Figure 13d shows a comparison in Per Unit (PU) of the inertial power of the small generator against the power output in PU of the VSC-HVDC system. As seen in Figure 13d, the magnitude and shape of the inertial power of the small generator is replicated with minimum change by the VSC-HVDC when GRF is enabled. These simulations assume zero delay in the transmission of the power command to the PAC-controlled wind farm.

5.2. Effects of Time Delay in the PAC-controlled Wind Farm

If time delay is included in the simulation, and no instantaneous energy extraction from the DC capacitor takes place, then the delayed response of the wind farm to a frequency excursion event produces an instability mode, with the medium size generator connected at the point of common coupling of the offshore wind farm, as seen in Figure 14. This shows the need to compensate for the

delay in communications using a feedforward loop in the onshore HVDC system to provide immediate artificial inertial response in a frequency event.

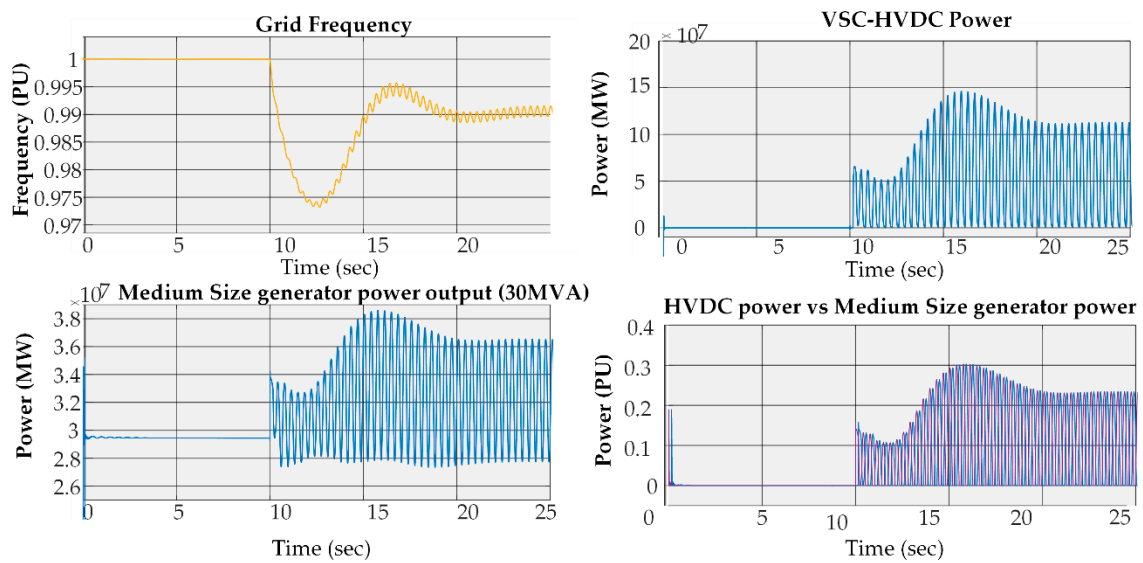


Figure 14. Effects of a 150ms delay in the PAC-controlled wind farm using the GRF concept.

5.3. Evaluation of the Generator Response Following Concept Assuming Constant Wind Speed and Communication Delay with Feedforward Controller

Figure 15 shows the behaviour of the multi-machine system during a frequency excursion with the GRF controller with feedforward for a case of a communication delay of 150ms. As seen in Figure 15b, the power output of the HVDC station follows the behavior of the medium size generator in a stable manner. The communication delay makes the power from the offshore wind farm lag with respect to the GRF command. However, the power output of the HVDC station is immediate, as seen in the graph of HVDC power at the onshore station vs. the wind farm power in Figure 15d.

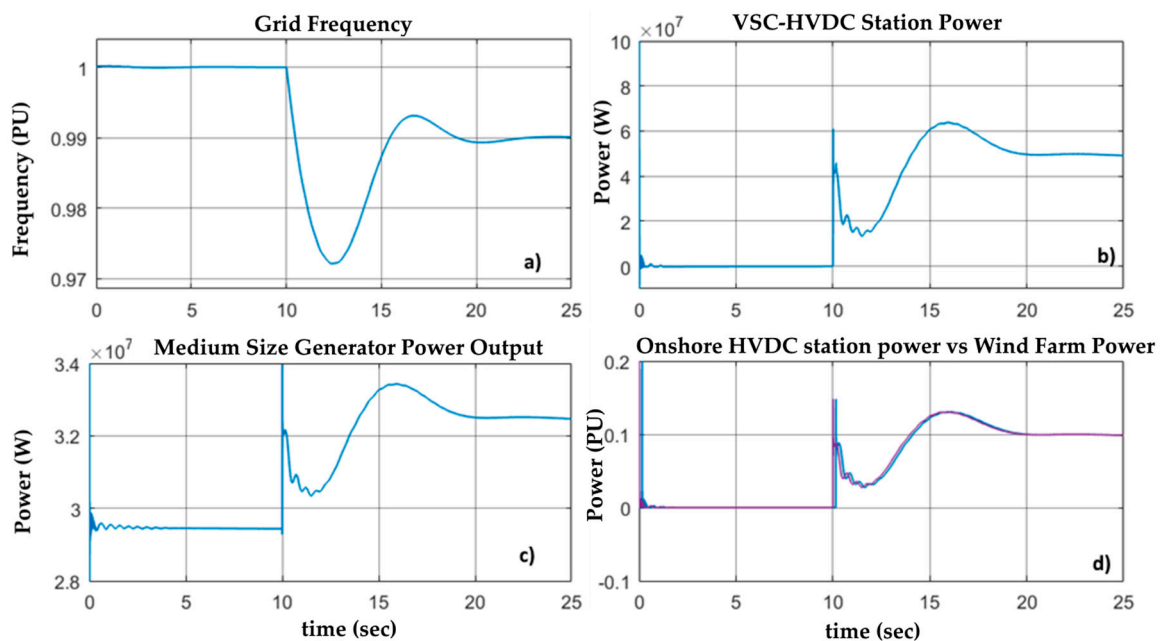


Figure 15. Behaviour of the multi-machine model for Generator Response Following concept control with communication delay of 150ms and feedforward controller.

To enable the immediate action of the onshore HVDC station during a frequency event, the feedforward controller extracts energy from the DC capacitors and injects it into the AC grid. Figure 16 shows a comparison between a GRF controller action for the system with no communication delay and for the system with communication delay of 150 ms.

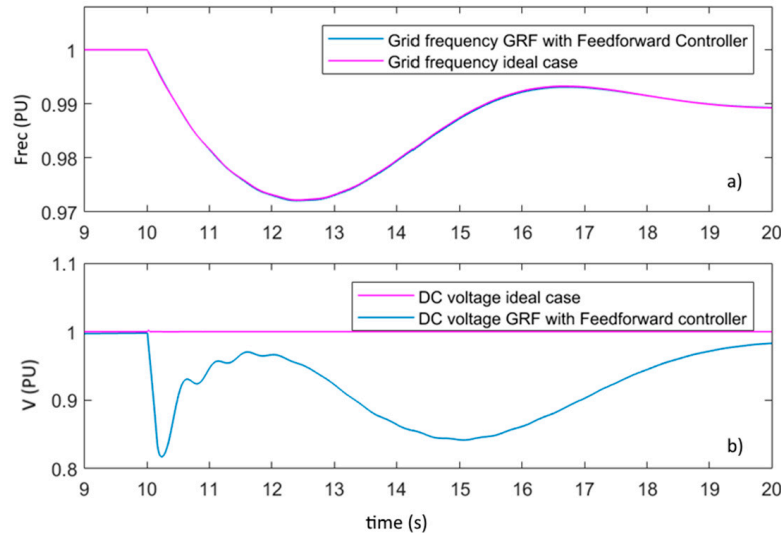


Figure 16. Comparison of HVDC DC voltage for a GRF action with no delay and with communication delay. (a) Grid frequency (b) HVDC voltage.

As seen in Figure 16a, the frequency response in both cases is very similar thanks to the action of the feedforward controller in the case of a delay in communications. The action of the feedforward controller affects the magnitude of the DC voltage, as seen in Figure 16b; however, the DC voltage reduction does not compromise the proper functioning of the HVDC converter.

5.4. Evaluation of the Generator Response Following Concept Assuming Variable Wind Speed and Communication Delay with Feedforward Controller

Having variable wind power generation implies having continuous power adjustments from all the generators to keep the grid frequency constant. Each generator supplies power to the grid based on their droop controller and governor constants. The small–medium generator of the GRF concept will also change its power output based on the change in wind power provision. Since the GRF concept is designed to function only during major frequency perturbations, the GRF controller implements an actuation threshold value and the controller constant of the small–medium machine governor (specially the droop constant) were selected to reduce the sensitivity of the governor for small frequency excursions.

To demonstrate the action of the controller under variable wind speed conditions, Figure 17 shows the behaviour of the GRF multi-machine test model when a sudden loss of a generator at $t = 10$ s produces a sudden frequency drop.

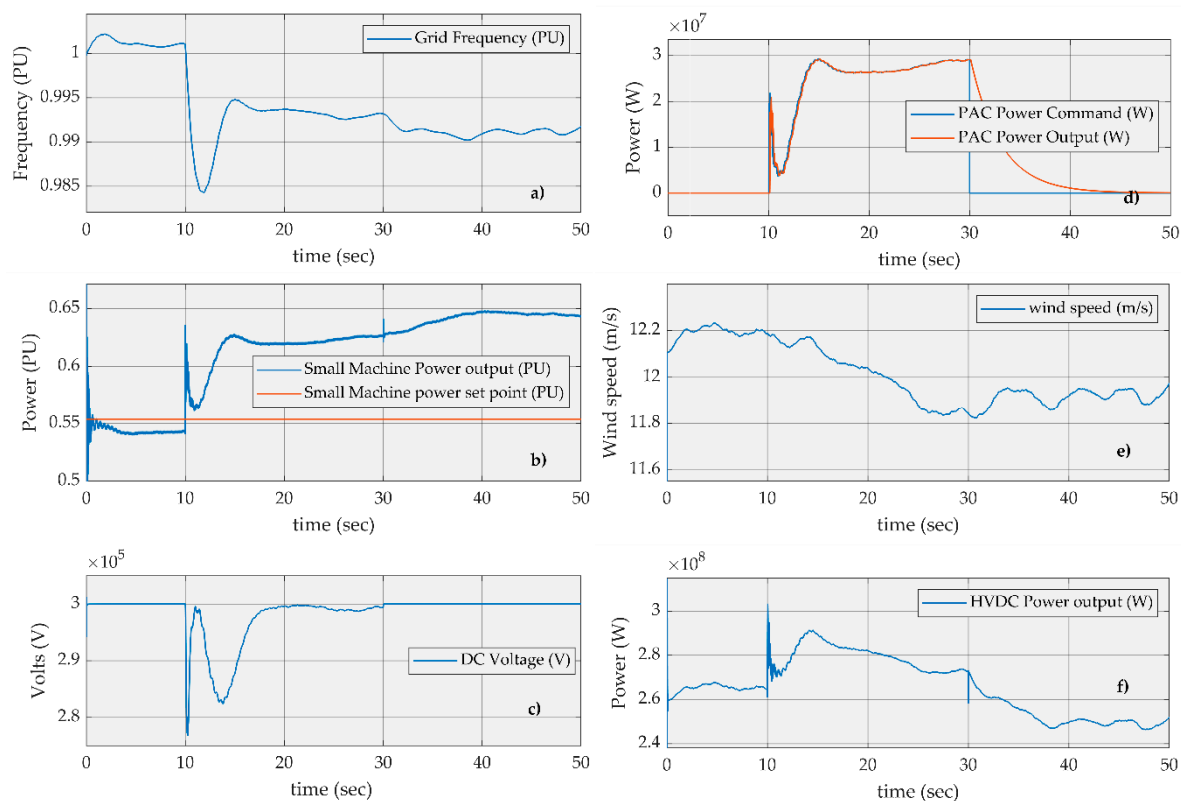


Figure 17. Behaviour of the multi-machine system with a variable wind power input and the GRF controller.

As seen in Figure 17a, the frequency of the grid is affected by the variability in wind power provision. At $t = 10$ s, the frequency drops, triggering an inertial and governor response from the small machine of the system, as seen in Figure 17b. Figure 17b shows that the small machine is working close to its set point prior to the frequency excursion. The small difference between the small machine power output and its reference point is due to the droop control in the machine governor. When a frequency excursion happens, the DC capacitor of the onshore VSC-HVDC substation injects some active power to the grid by command of the feedforward controller. This causes the DC voltage to oscillate following the feedforward power provision command, as seen in Figure 17c. Figure 17d shows the power output command from the GRF controller in blue. The PAC controller, as seen in the red plot in Figure 17d, applies this power output command (after a short delay because of the communication channel). The GRF power command lasts for 20 seconds. After this, the power signal command resets and the PAC controller gradually decreases its power output following its internal dynamics. Finally, Figure 17f shows the power output of the VSC-HVDC system. This power output includes the energy provided by the GRF (i.e., the feedforward controller and the PAC) and the wind power.

Figure 18 shows a comparison of the behaviour of a multi-machine system when the GRF controller is enabled vs. when the GRF controller is disabled. The simulation with the GRF controller active is shown in blue and the simulation with the inactive GRF is shown in red.

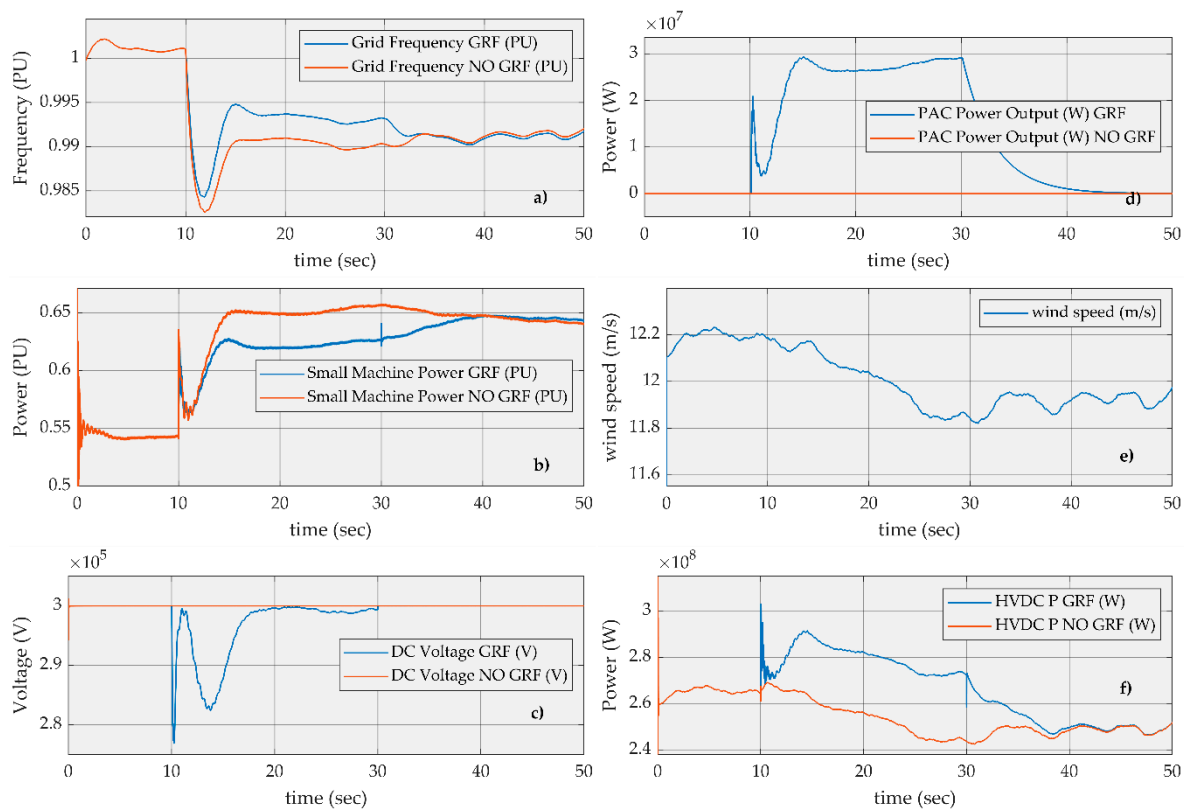


Figure 18. Comparison of the multi-machine system dynamics when the GRF controller is enabled/disabled.

As seen in Figure 18a, when the GRF controller is active, the frequency profile of the grid is improved by the extra power provided by the PAC-controlled offshore wind farm. Figure 18b shows the power output of the small machine. Here, when the GRF is active, the extra power provided to the grid by the offshore wind farm reduces the governor response of the small machine. When the GRF is inactive, the small machine is forced to provide more power output to try to compensate for the frequency drop. Figure 18c shows the voltage profile of the HVDC link. When the GRF controller is active (blue plot), the feedforward action of the controller extracts energy from the DC capacitor to compensate for the delay in power provision from the PAC-controlled offshore wind farm. This action makes the DC voltage fluctuate; however, this fluctuation is within the safe margin of operation of the HVDC system. The feedforward controller enforces this margin. Figure 18d shows the extra power output of the wind farm driven by the PAC controller. When the GRF is active, the PAC provides a power output following the power profile of the small machine, as seen in the blue plot. When the GRF is inactive, the PAC commands no extra power provision from the wind farm, as shown in the red plot. Finally, Figure 18f shows the power output of the HVDC system. This power output follows the profile of the wind model. When GRF is active, the HVDC power includes the energy provided by GRF during frequency excursions (i.e., the feedforward controller and the PAC) and the wind power. When GRF is inactive, the HVDC power output is just the wind power minus the transmission and conversion losses.

Figure 19 is provided to evidence the accuracy of the GRF controller in following the behaviour of a governor-controlled medium-sized machine and the effects of modifying the control constant of the machine governor.

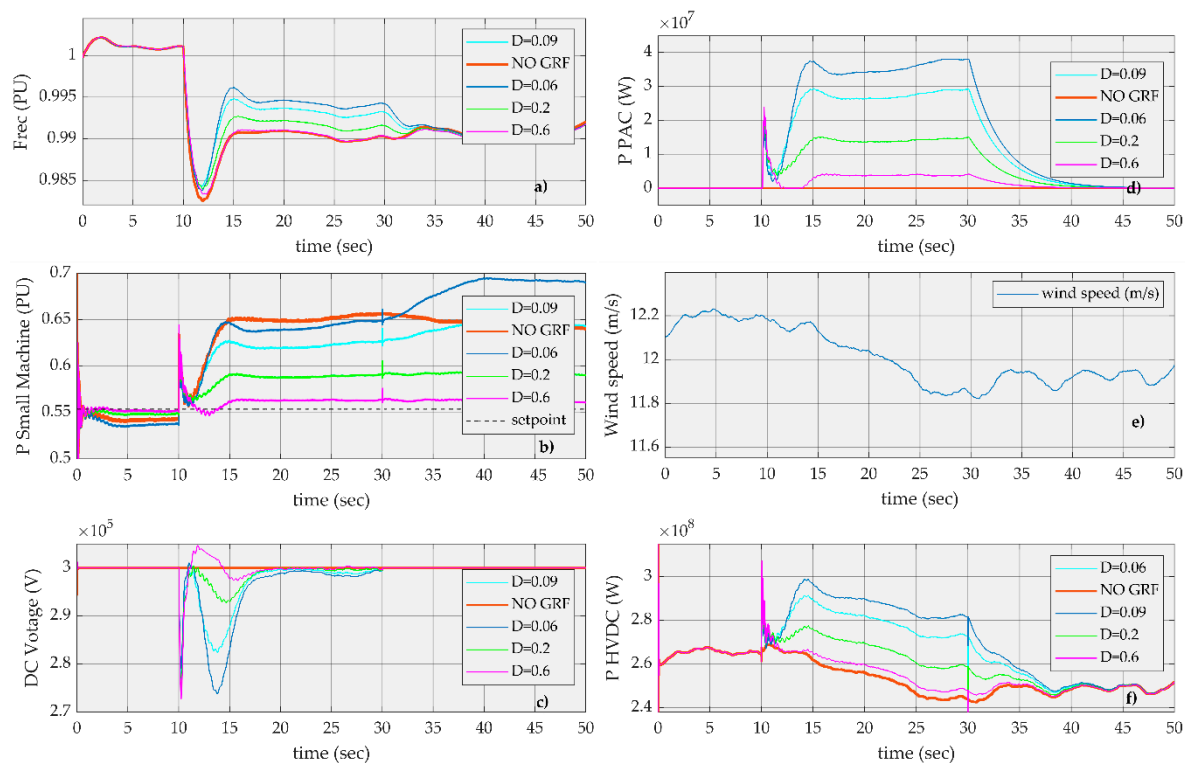


Figure 19. Effects of different droop control constants in the small generator when using the GRF controller.

As seen in Figure 18, the governor droop constant (D) is selected to be 0.06 (most sensitive to frequency variation), 0.09, 0.2 and 0.6 (least sensitive to frequency variations). Figure 19 shows the effects of changing D on the grid frequency (Figure 19a), the power output of the small machine (Figure 18b), the HVDC dc voltage (Figure 19c), the power provided by the PAC controller (Figure 19d) and the HVDC power output (Figure 19f). As seen in the plot in Figure 19, the GRF controller is able to follow the small generator over a wide range of governor settings. Another conclusion obtained from Figure 19a,b is that the immediate power output response of the small generator during a frequency excursion is mostly based on its internal dynamics and not on the governor constants. As such, if GRF is used to reduce the initial frequency drop of the grid, then the gain of the GRF controller should be increased. The effects of doing this are shown in Figure 20.

Figure 20 shows the effect of changing the GRF controller gain with a small generator with 0.1 droop constant. The gain of the GRF controller defines the magnitude of the extra energy provision from the PAC-controlled wind farm and is obtained by multiplying the small generator power output in PU by a MW-defined gain G . The values of G defined for the simulation are 100MW, 300MW and 400MW. Figure 20 shows the effects of changing G in the grid frequency (Figure 20a), the power output of the small machine (Figure 20b), the HVDC dc voltage (Figure 20c), the power provided by the PAC controller (Figure 20d) and the HVDC power output (Figure 20f). As seen in Figure 20a, the impact of the loss of generation in the grid frequency decreases for higher values of G . Although the frequency response is similar to the cases presented in Figure 19, changing the value of G instead of D has other effects on the rest of the variables of the system (such as the DC voltage). The tuning of the G and D variables must be carried out based on the power handling capacities of the PAC-controlled wind farm and the desired dynamic response of the HVDC system. Proper tuning of the G and D variables can maximize the advantages of the GRF controller and further improves the frequency performance of the grid.

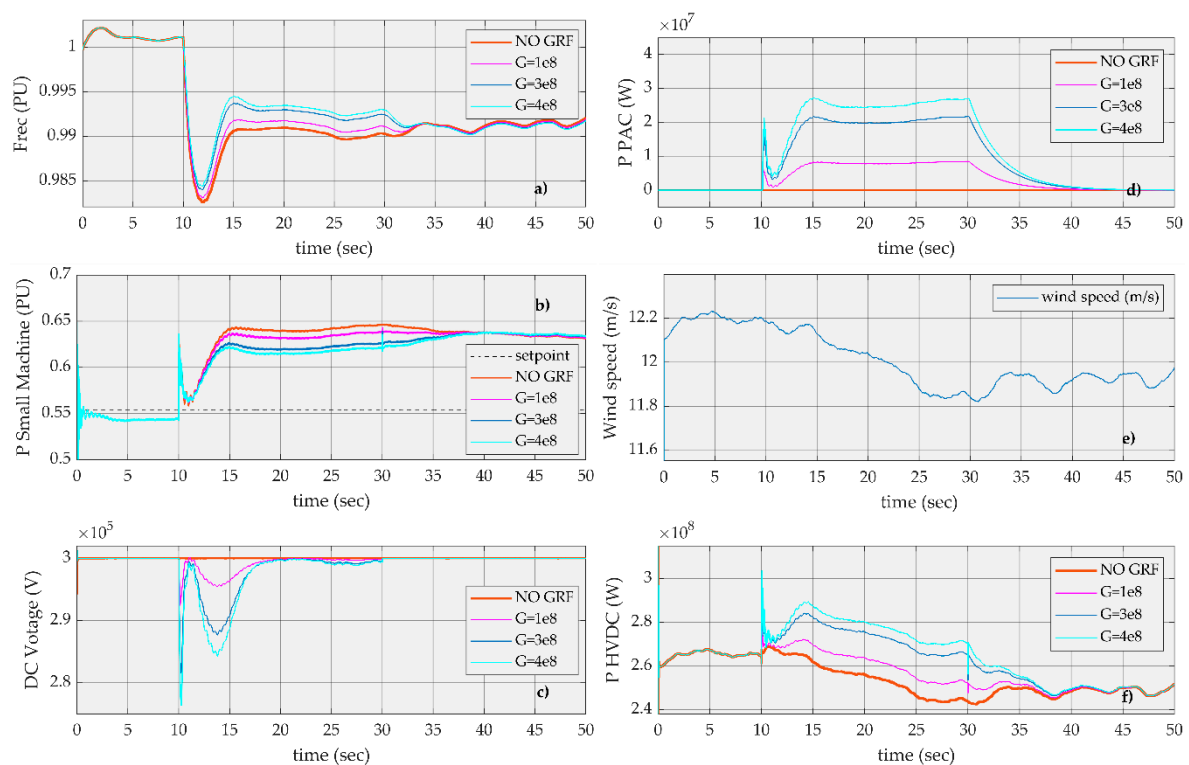


Figure 20. Effect of different gain values when using the GRF controller.

6. Conclusions

The GRF concept presented in this paper offers a novel and timely solution to the ever-increasing need to develop systems that are compatible with the operation of classic power systems. The innovation potential is significant when considering that industry, academia and utilities have repeatedly expressed the need for tools and strategies, such as the one presented in this paper, to enable the large-scale integration of wind power to the electric system.

Whilst the research efforts of this project focused on the development of a feedforward controller to handle communication delays, there is still a lot of room to improve the response the offshore wind farm to reduce the fluctuations in the HVDC voltage transients and minimize the disturbances to the feedforward controller. Additionally, the controllers developed herein require further validation in low-power experimental setups. These tasks can be covered in future iterations of the project.

Author Contributions: Conceptualization, O.A.-L. and W.L.; methodology, D.C.-G., O.A.-L., W.L.; software, D.C.-G.; validation, D.C.-G., formal analysis, D.C.-G., O.A.-L., W.L.; investigation, D.C.-G.; resources, D.C.-G., A.S.; writing—original draft preparation, D.C.-G., A.S., O.A.-L.; writing—review and editing, D.C.-G., A.S., O.A.-L., W.L.; supervision, O.A.-L. and W.L.; project administration, O.A.-L. and W.L.; funding acquisition, O.A.-L. and W.L. All authors have read and agreed to the published version of the manuscript.

Funding: This research was funded by the Engineering and Physical Sciences Research Council (EPSRC) SUPERGEN Wind Programme under Grant EP/L014106/1.

Conflicts of Interest: The authors declare no conflict of interest.

References

1. Bjerge, C.; Kristoffersen, J.R. How to run an offshore wind farm like a conventional power plant. *Mod. Power Syst.* **2007**, *27*, 31–33.
2. Knudsen, T.; Bak, T.; Svenstrup, M. Survey of wind farm control-power and fatigue optimization. *Wind Energy* **2014**, *18*, 1333–1351. [[CrossRef](#)]
3. Anaya-Lara, O.; Hughes, F.; Jenkins, N.; Strbac, G. Contribution of DFIG-based wind farms to power system short-term frequency regulation. *IEE Proc.-Gener. Transm. Distrib.* **2006**, *153*, 164–170. [[CrossRef](#)]

4. Stock, A.; Leithead, W.E. Providing grid frequency support using variable speed wind turbines with augmented control. In *EWEA2014*; European Wind Energy Association: Barcelona, Spain, 2012.
5. Hur, S.-H.; Leithead, W.E. Curtailment of wind farm power output through flexible turbine operation using wind farm control. In *EWEA2014*; European Wind Energy Association: Barcelona, Spain, 2014.
6. Stock, A. Augmented Control for Flexible Operation of Wind Turbines. Ph.D. Thesis, University of Strathclyde, Glasgow, UK, 6 July 2015.
7. Stock, A.; Leithead, W.E. Providing frequency droop control using variable speed wind turbines with augmented control. In *EWEA2014*; European Wind Energy Association: Barcelona, Spain, 2014.
8. Leferink, F.; Keyer, C.; Melentjev, A. Static energy meter errors caused by conducted electromagnetic interference. *IEEE Electromagn. Compat. Mag.* **2016**, *5*, 49–55. [[CrossRef](#)]
9. Roscoe, A.J.; Dyško, A.; Marshall, B.; Lee, M.; Kirkham, H.; Rietveld, G. The Case for Redefinition of Frequency and ROCOF to Account for AC Power System Phase Steps. In Proceedings of the 2017 IEEE International Workshop on Applied Measurements for Power Systems (AMPS), Liverpool, UK, 20–22 September 2017; pp. 1–6.
10. Florencias-Oliveros, O.; Agüera-Pérez, A.; Sierra-Fernández, J.; González-De-La-Rosa, J.; Palomares-Salas, J.; Espinosa-Gavira, M. Voltage Supply Frequency Uncertainty influence on Power Quality index: A qualitative analysis of Higher-Order Statistics 2D trajectories. In Proceedings of the 2018 IEEE 9th International Workshop on Applied Measurements for Power Systems (AMPS), Bologna, Italy, 26–28 September 2018; pp. 1–6.
11. Hogg, S. *UK Wind Energy Technologies*; Routledge: Oxon, UK, 2016.
12. Jamieson, P. *Innovation in Wind Turbine Design*; Wiley: Hoboken, NJ, USA, 2011.
13. Campos-Gaona, D.; Pena-Alzola, R.; Ordonez, M. Non-Minimum Phase Compensation in VSC-HVDC Systems for Fast Direct Voltage Control. *IEEE Trans. Power Deliv.* **2015**, *30*, 1. [[CrossRef](#)]
14. Morari, M.; Zafiriou, E. *Robust Process Control*; Prentice-Hall: Upper Saddle River, NJ, USA, 1989.
15. Wang, Q.-G.; Bi, Q.; Zhang, Y. Partial internal model control. *IEEE Trans. Ind. Electron.* **2001**, *48*, 976–982. [[CrossRef](#)]
16. Campos-Gaona, D.; Moreno-Goytia, E.L.; Anaya-Lara, O. Fault Ride-Through Improvement of DFIG-WT by Integrating a Two-Degrees-of-Freedom Internal Model Control. *IEEE Trans. Ind. Electron.* **2012**, *60*, 1133–1145. [[CrossRef](#)]



© 2020 by the authors. Licensee MDPI, Basel, Switzerland. This article is an open access article distributed under the terms and conditions of the Creative Commons Attribution (CC BY) license (<http://creativecommons.org/licenses/by/4.0/>).